REPORT DOCUMENTATION PAGE		Form Approved OMB NO. 0704-0188

1. REPORT DATE (DD-MM-YYYY) 21-07-2017	2. REPORT TYPE Final Report	3. DATES COVERED (From - To) 25-Sep-2016 - 24-Jun-2017

4. TITLE AND SUBTITLE
Final Report: Direct Measurement of Electron Mobility in Carbon-Nanocatalyst Composites

5a. CONTRACT NUMBER
W911NF-16-1-0581

5b. GRANT NUMBER

5c. PROGRAM ELEMENT NUMBER
611102

6. AUTHORS
Aruni Gankanda, Mojtaba Abolhassani, Lauren F. Greenlee

5d. PROJECT NUMBER

5e. TASK NUMBER

5f. WORK UNIT NUMBER

7. PERFORMING ORGANIZATION NAMES AND ADDRESSES
University of Arkansas
210 Administration Building
1 University of Arkansas
Fayetteville, AR   72701 -1201

8. PERFORMING ORGANIZATION REPORT NUMBER

9. SPONSORING/MONITORING AGENCY NAME(S) AND ADDRESS (ES)

U.S. Army Research Office
P.O. Box 12211
Research Triangle Park, NC 27709-2211

10. SPONSOR/MONITOR'S ACRONYM(S)
ARO

11. SPONSOR/MONITOR'S REPORT NUMBER(S)
69805-CH-II.1

12. DISTRIBUTION AVAILIBILITY STATEMENT
Approved for Public Release; Distribution Unlimited

13. SUPPLEMENTARY NOTES
The views, opinions and/or findings contained in this report are those of the author(s) and should not contrued as an official Department of the Army position, policy or decision, unless so designated by other documentation.

14. ABSTRACT
The goal of the research was to demonstrate direct measurement of electron mobility in graphene and graphene-nanoparticle composite materials. It is thought that electron transfer between catalytic nanoparticles and a conductive substrate such as graphene is an important mechanism for chemical reactivity in aqueous systems. However, to date, there has been no direct measurement of this electron transfer mechanism. During the course of this project, successful development of an experimental setup for demonstrated direct measurement of electron mobility via the Hall effect was accomplished, as well as synthesis of graphene oxide and control of graphene oxide

15. SUBJECT TERMS
electron mobility, conductivity, graphene, nanoparticles, electron transfer, Hall measurement

16. SECURITY CLASSIFICATION OF:			17. LIMITATION OF ABSTRACT	15. NUMBER OF PAGES	19a. NAME OF RESPONSIBLE PERSON Lauren Greenlee
a. REPORT UU	b. ABSTRACT UU	c. THIS PAGE UU	UU		19b. TELEPHONE NUMBER 610-507-6390

Agency Code:

Proposal Number: **Agreement Number:**

Organization:
Address: , ,
Country:
DUNS Number: EIN:
Report Date: Date Received:
 for Period Beginning and Ending
Title:
Begin Performance Period: **End Performance Period:**
Report Term: -
Submitted By: Email:
                                                             Phone:

Distribution Statement: -

STEM Degrees: **STEM Participants:**

Major Goals:

Accomplishments:

Training Opportunities:

Results Dissemination:

Plans Next Period:

Honors and Awards:

Protocol Activity Status:

Technology Transfer:

<u>Table of Contents: Direct Measurement of Electron Mobility in Carbon-Nanocatalyst Composites</u>

Objective 1:   Develop 4-point contact electrode setup and graphene-Fe NP deposition technique

Objective 2: Determine the conductivity, electron mobility, and electron carrier concentration of individual graphene slices

Final Report for:

STIR: Direct Measurement of Electron Mobility in Carbon-Nanocatalyst Composites

Aruni Gankanda, Mojtaba Abolhassani, Shelby Foster, Sergio Bakovic, Lauren F. Greenlee

University of Arkansas, Fayetteville, AR, USA

This project focused on successful experimental demonstration of Hall measurement, which allows direct measurement of the electron mobility and electron carrier concentration of a material, on graphene and nanoparticle-immobilized graphene substrates. While Hall measurement is used extensively in the semi-conductor research field to understand the electronic properties of materials, Hall measurement has only recently been applied to other materials such as graphene and there are still great challenges and questions to be answered with these measurements. Further, to our knowledge, no one has directly probed how the electronic properties of conductive materials such as graphene and catalytic nanoparticles impact aqueous chemistry environments. Thus, we report on the key experimental steps we have taken to demonstrate successful direct measurement of the electronic properties of single-layer graphene and nanoparticles immobilized on graphene utilizing the physics-based measurement of Hall voltage. The results reported herein represent the preliminary work needed to establish appropriate and viable experimental methods for sample preparation as well as report on our initial Hall measurement results.

Project Research Activities and Results

<u>Objective 1</u>: Develop 4-point contact electrode setup and graphene-Fe NP deposition technique.

1.1 Graphene and Graphene Oxide Sample Development

1.1.1 Graphene

Monolayer and bilayer graphene samples deposited on a 5x5 mm^2 Si/SiO$_2$ wafer with a 300 nm SiO$_2$ layer were purchased form Graphenea. Theoretical thickness of the monolayer and bilayer graphene layers was 0.345 and 0.69 nm, respectively.

1.1.2 Synthesis of Graphene Oxide (GO) and Reduced Graphene(rGO) Oxide and Transferring onto Silicon Wafers

a) Graphene Oxide

Graphene oxide samples were synthesized in the lab by graphite exfoliation using the modified Hummers method. However, the graphene oxide samples obtained from traditional modified Hummers method approaches were contaminated with graphite due to incomplete oxidation. Therefore, the amount of graphite in the reaction mixture and reaction times were optimized to obtain clean single-layer graphene oxide samples suitable for Hall measurement studies. The experimental procedure of the optimized modified hummers method is as follows (Figure 1).

Concentrated sulfuric acid (23 ml) was mixed with 0.5 g of graphite powder and stirred for 1 h in an ice bath. At this stage, graphite is converted to graphite intercalated with anions and water. Then 3 g of potassium permanganate was added into the sulfuric acid, graphite mixture in very small amounts and continued stirring for 1 h. Then the mixture was heated to 40 ˚C and continued stirring at this temperature for 3 h for the oxidation of graphite. The actual oxidant of this reaction

was manganese heptoxide (Mn_2O_7), formed by the reaction of potassium permanganate with sulfuric acid (Reaction 1 to 3).
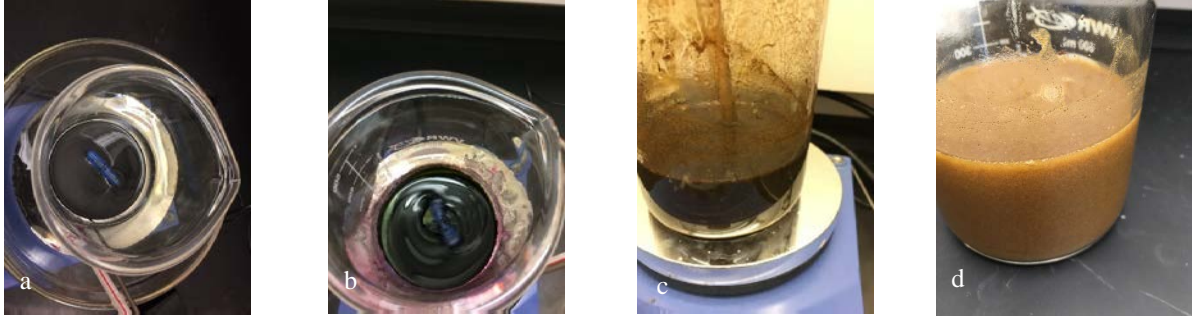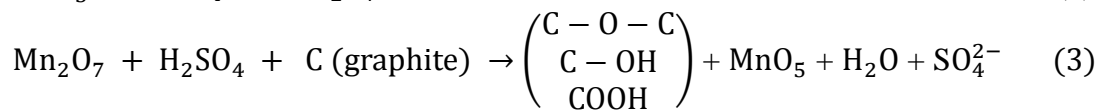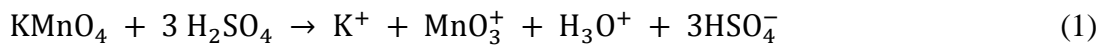

Figure 1. Synthesis of graphene oxide a) mixture of 0.5 g graphite and 23 ml of H_2SO_4 stirring in an ice bath (black) b) H_2SO_4 and graphite mixture after the addition of potassium permanganate (green) c) mixture in step (b) after heating at 40 ℃ for 3 h (dark brown-oxidized graphite) d) oxidation mixture after the addition of 160 mL of water followed by 6 ml hydrogen peroxide (light brown-exfoliated graphene oxide).

Next, this mixture was heated to 95˚C while slowly adding 160 mL of water to exfoliate the oxidized graphite (pristine graphite oxide) into graphene oxide. The final step was slow addition of 6 mL of hydrogen peroxide in order to complete the oxidation. X-ray diffraction (XRD) analysis results of the graphene oxide samples synthesized from different methods are shown in Figure 2a. This result clearly shows that the graphene oxide synthesized by the optimized method is free of graphite. Figure 2b shows a SEM image of exfoliated graphite using our optimized Hummers method.
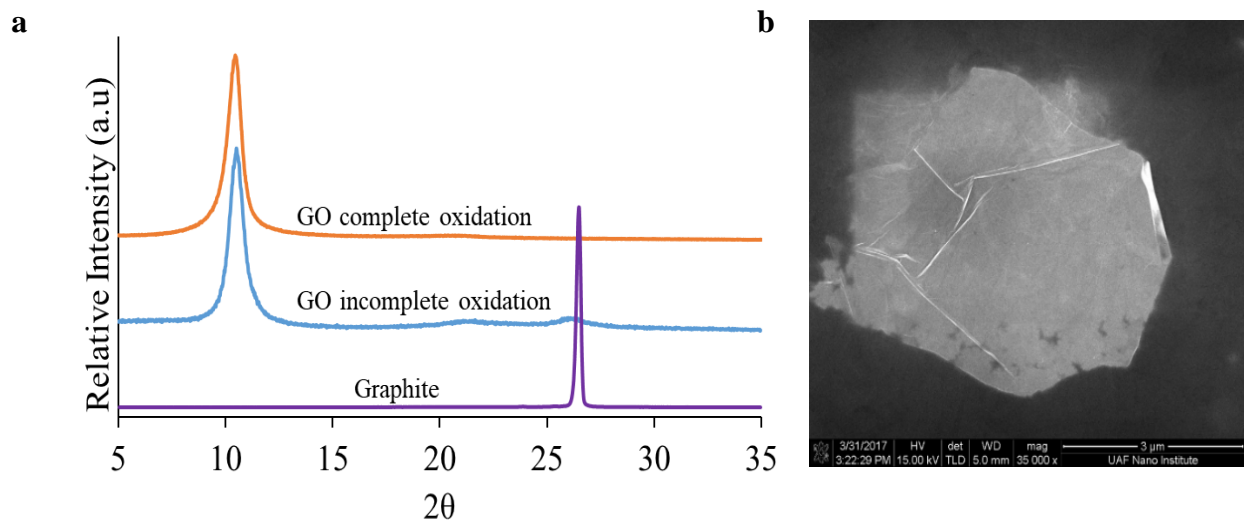
$$KMnO_4 + 3 H_2SO_4 \rightarrow K^+ + MnO_3^+ + H_3O^+ + 3HSO_4^- \qquad (1)$$

$$MnO_3^+ + MnO_4^- \rightarrow Mn_2O_7 \qquad (2)$$

$$Mn_2O_7 + H_2SO_4 + C \text{ (graphite)} \rightarrow \begin{pmatrix} C-O-C \\ C-OH \\ COOH \end{pmatrix} + MnO_5 + H_2O + SO_4^{2-} \qquad (3)$$

Figure 2. Characterization of exfoliated graphite a) comparison of XRD spectra of graphite produced by ordinary modified Hummers method and optimized Hummers method with graphite b) SEM image of exfoliated graphite by optimized Hummers method.

b) Reduced Graphene Oxide

Reduced graphene oxide was prepared by reduction of graphene oxide with sodium borohydride. In the reduction, 25 mg of GO was dispersed in 15 ml of 300 mM sodium borohydride and reacted for 24 h. Reduced graphene oxide synthesized in this way has a similar structure to graphene. The XRD feature centered at $21.5°$ confirms formation of reduced graphene oxide (Figure 3b). Also the color of graphene oxide is brownish while dried reduced graphene oxide is more blackish in color.
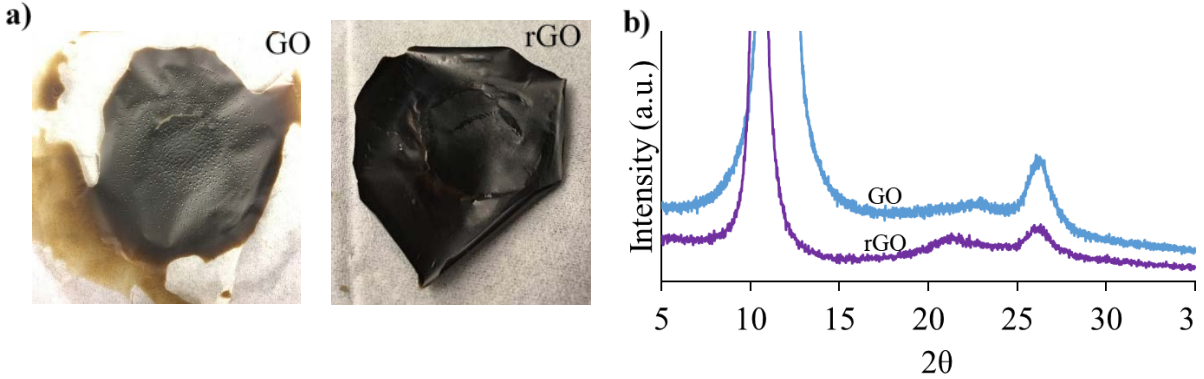

Figure 3. Comparison of graphene oxide (GO) and reduced graphene oxide (rGO) a) Images showing the brown color of GO changing to black upon conversion to rGO b) XRD patterns of GO and rGO.

c) Transferring Graphene Oxide onto Silicon Wafers

In the current study, graphene oxide was transferred onto 5x5 mm^2 silicon wafers with a 300 nm silicon dioxide layer by drop casting or spray coating. Water and water-methanol mixtures were used as the dispersion medium. Due to high surface tension of water, graphene oxide dispersed in

water was unable to create a thin film of oxide on the wafer. This problem was circumvented by using a 9:1; methanol: water mixture and heating the wafer to 80 ˚C prior to coating the graphene oxide sample on the wafer. Heating helped rapid evaporation of solvent. Further, optical microscopic images revealed that spray coating is much better in creating uniform films than drop casting (Figure 4). A solid loading of 20 mg GO per 5 ml of solvent was used in all of the above experiments.

1.1.3 Experimental Approaches to Contact Deposition

Contact deposition on the graphene samples on the Si/SiO_2 wafer was done in two ways. The first method of contact deposition was direct soldering of Indium on four corners of the sample. In this method, Indium was cut into four small pieces using a razor blade while observing the sample under a microscope. Indium contacts were pushed to each corner of the sample with tweezers and annealed for two minutes. Then gold wires were attached on contacts using epoxies (Figure 5). Contacts made via this method had high resistance, and therefore sometimes the samples were not suitable to be used for accurate Hall measurements.

Drop casting · Spray coating

Figure 4. Optical microscopy images of graphene oxide transferred on to Si/SiO_2 wafer by drop casting and spray coating. Solvent is 9:1, methanol:water.

Therefore, in later experiments, Ti (5nm)/Au(100 nm) electrical contacts of 0.5x0.5 mm^2 were deposited on four corners of the sample in the Van der Pauw geometry using photolithography (Figure 6). AZ 4330 and AZ400k were used as the photoresist and developer, respectively.
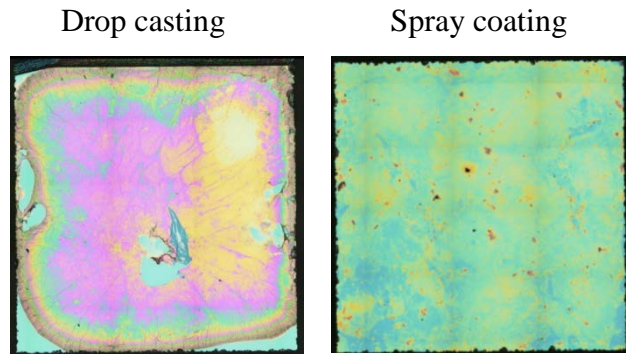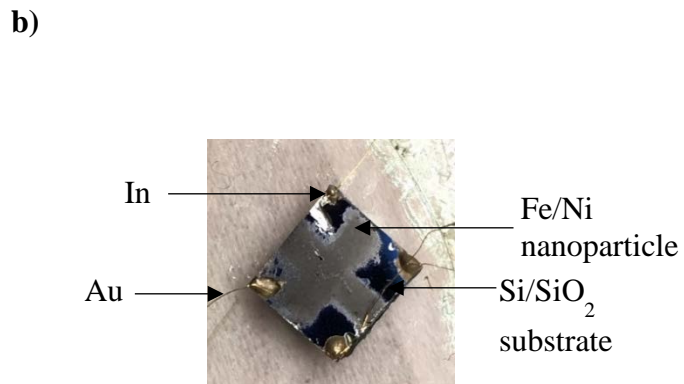

Figure 5. a) Annealing of Indium contacts b) Graphene sample with Indium contacts and gold wires attached to the contacts with epoxy.
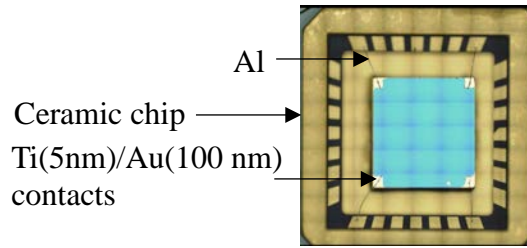
Figure 6. Monolayer graphene sample with Ti/Au contacts mounted on a chip carrier by wire bonding.

Contacts deposited with photolithography are uniform in size and thickness, and also these features were highly reproducible for different samples. The main challenge during photolithography was to retain the monolayer or bilayer of graphene on silicon wafer intact. Therefore, sonication was avoided in all the steps of contact deposition procedure. As an alternative to sonication, photoresist on the graphene sample was dipped in acetone for a longer time to remove the photoresist after contact deposition. Lift off of the photoresist was monitored by observing under an optical microscope.

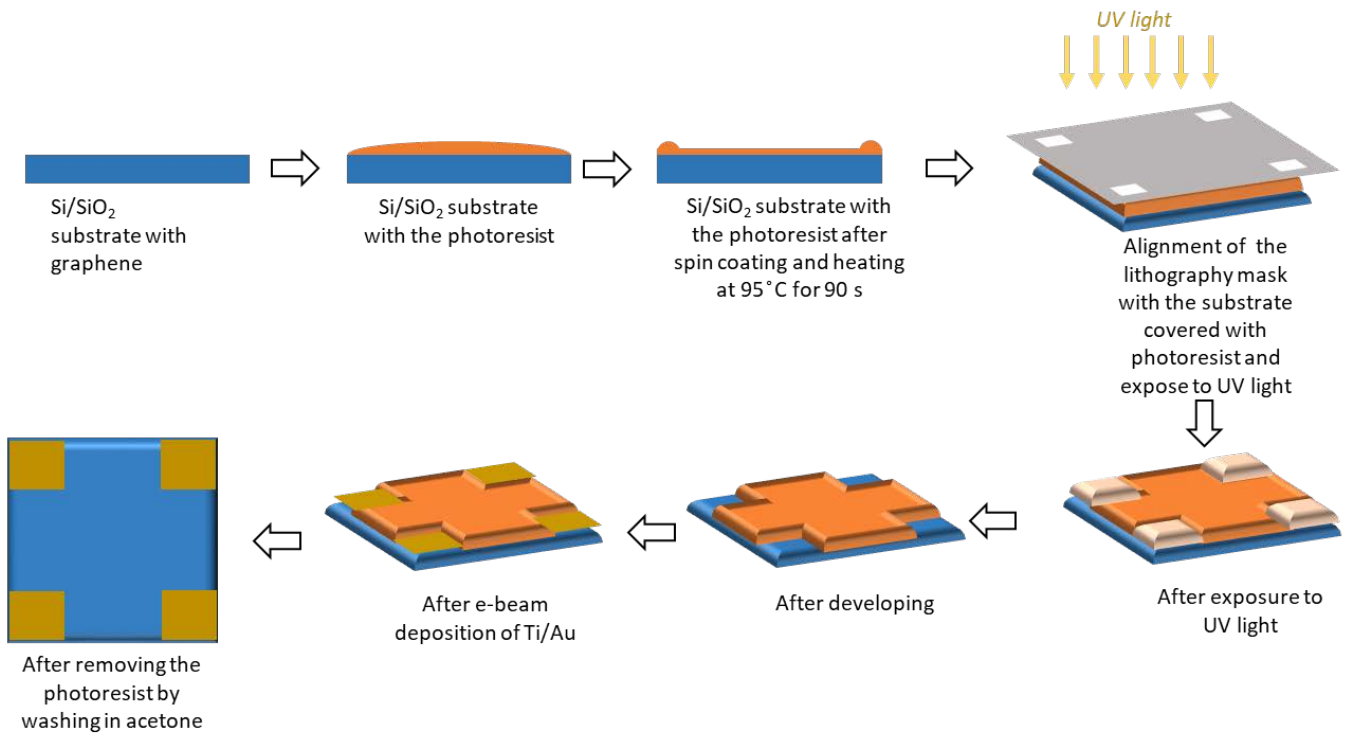A summary of the photolithography procedure is shown in Figure 7.

Figure 7. Contact deposition on graphene samples using photolithography.

1.1.4. Sample Characterization

Graphene layers deposited on silicon wafers are subjected to extensive processing during photolithography. Therefore, all the graphene samples were characterized by Raman spectroscopy before and after photolithography (Figure 8). The presence of characteristic G and 2D bands in Raman spectra confirmed the presence of graphene even after photolithography.
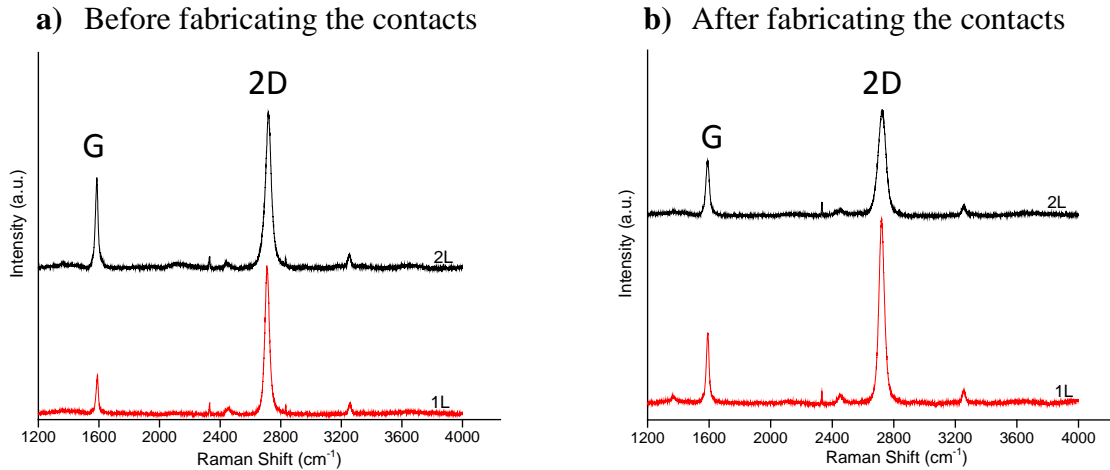
a) Before fabricating the contacts   **b)** After fabricating the contacts

Figure 8. Characterization of graphene samples before and after contact deposition with Raman spectroscopy. Black = bi-layer; Red = mono-layer.

Objective 2: **Determine the conductivity, electron mobility, and electron carrier concentration of individual graphene slices.**

2.1. Hall Setup

In Hall measurements (Figure 9), the material to be evaluated is placed in a magnetic field perpendicular to the direction of an applied current through conductor. As the current flows through the sample, charged particles (i.e., protons or holes and electrons) in a magnetic field experience a force which pushes the electrons to one side of the sample. As a result, a voltage is developed across the conductor in a direction normal to the direction of both the current and the magnetic field (Hall effect or Hall voltage). The extent to which the Hall effect takes place is related to the mobility of charge carriers. In the current study, hall measurements were done using this approach, which is also known as the Van der Pauw technique. The key features of the Van der Pauw technique include:
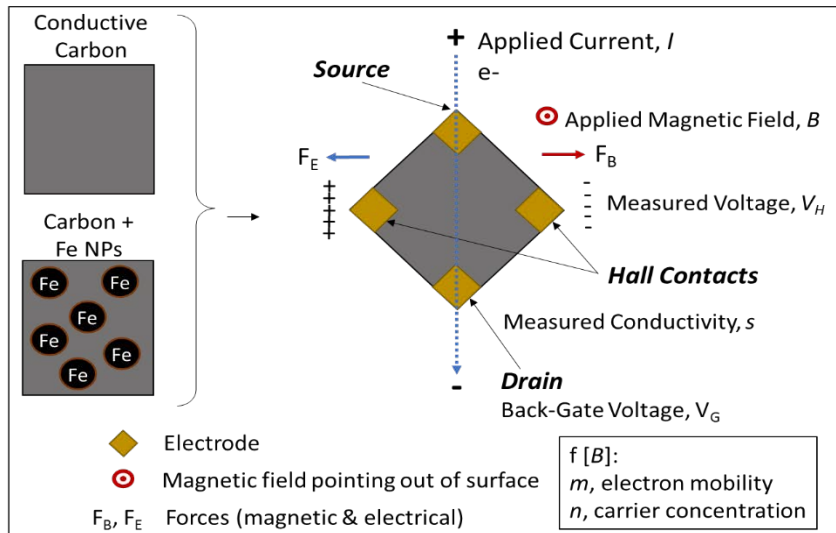
Figure 9. Hall measurement setup.

7

perpendicular magnetic field and measurement of the in-plane voltage (Hall voltage) that is established as a result of the magnetic field and the applied current.

2.2. Measurement Approach

2.2.1. Measurement of GaN

A 5x5 mm^2 GaN with a ~3 µm thickness was used to test the experimental procedure and the setup. The starting current was -500 µA and ramped up to 500 µA with 100 µA current steps. The magnetic field was varied from 0.5 to -0.5 T with a 0.1 T ramp. Hall measurements for the GaN sample were obtained with a Lakeshore 7500 system. All the measurements were performed at room temperature. As shown in Figure 10, the IV curve for GaN sample with In contacts resulted in a linear correlation that goes thorough the origin, which is expected ohmic behavior. Magnetic field vs Hall voltage curves also show typical linear behavior. However, the two lines do not show zero Hall voltage in the absence of a magnetic field due to the presence of an offset voltage.
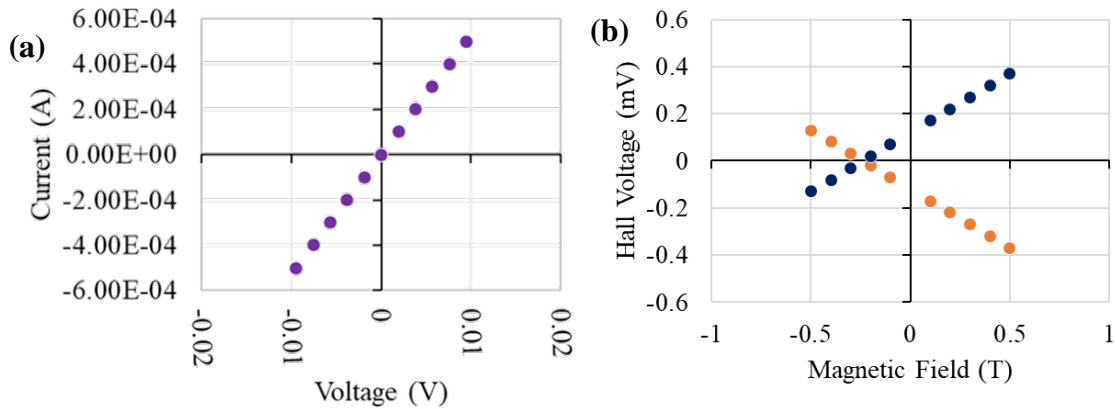

Figure 10. a) IV curve for GaN b) Hall measurements of GaN.

2.2.2. Measurement of Silicon substrate

Since the monolayer and bilayer graphene samples were grown on a Si/SiO$_2$ substrate, Hall measurements of a sample of silicon with 300 nm silicon dioxide were obtained as a control. A silicon wafer with 300 nm silicon dioxide layer of 5x5 mm^2 was used for measurements. Indium contacts were used to connect the sample to the Lakeshore 7500 Hall setup. As shown in Figure 11a, the IV curve obtained for of Si/SiO$_2$ showed non-ohmic behavior. The major reason for non-ohmic behavior is improper contacts. Change in the Hall voltage with the magnetic field also showed nonlinear behavior. Here we are only showing the Hall voltage obtained for positive magnetic fields for ease of comparison with the measurements of the graphene samples.
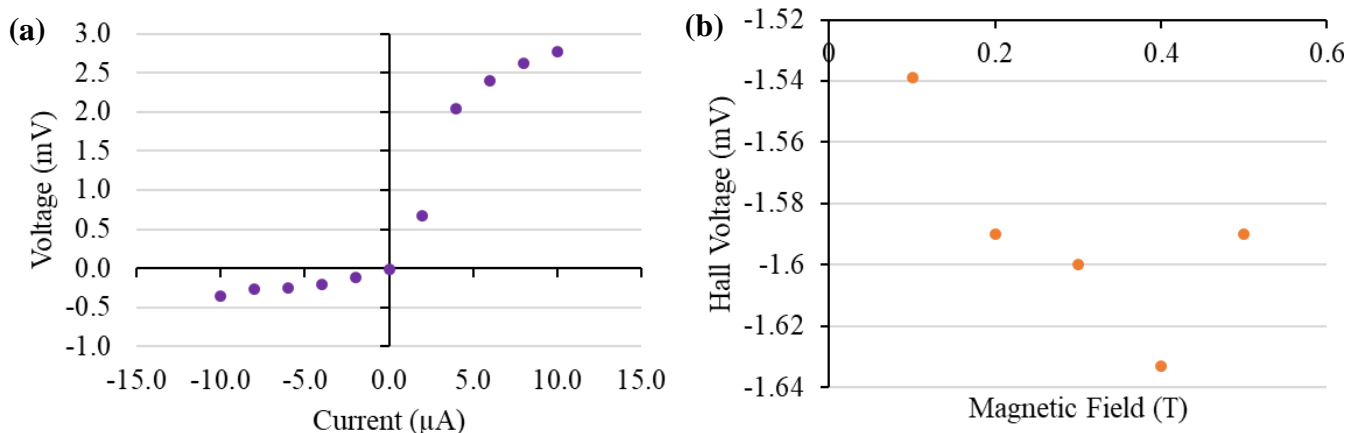
Figure 11. a) IV curve for Si/SiO$_2$ b) Hall measurements of Si/SiO$_2$.

2.2.3. Measurement of Monolayer Graphene

Monolayer graphene samples of 5x5 mm^2 were used for Hall measurements. Hall measurements and IV curves obtained for graphene with In contacts using the Lakeshore 7500 are shown in Figure 12. IV curve in Figure 12a shows ohmic behavior. However, as shown in Figure 12b, the Hall voltage did not vary linearly with the magnetic field as expected. A major reason for this type of measurement is high contact resistance. Therefore, Ti(5nm)/Au(100 nm) contacts of 0.5x0.5 mm^2 was fabricated on the graphene sample with photolithography. This sample was then mounted on a ceramic chip carrier and wire bonded with an Al wire. Then four Sn:Pb:Ag; 62:36:2 wires were soldered on the chip carrier in order to connect the sample to the Hall measurement setup. Hall measurements for these samples were performed at a 50 nA constant current and 0.05 to 0.2 T magnetic field.
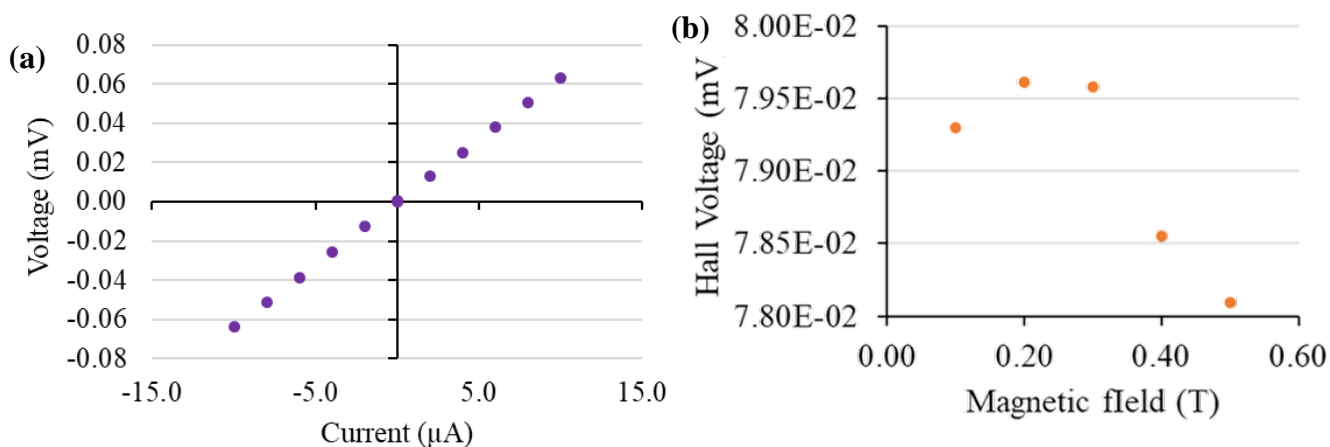

Figure 12. Graphene with In contacts a) IV curve b) Hall measurements.

Due to a mechanical problem in the Lakeshore 7500 system, Hall measurements for monolayer graphene samples with Ti/Au contacts were performed using a MMR hall measurement instrument. This instrument did not have the ability to measure IV curves within the low voltage

9

range required for our samples. Therefore, only Hall measurements were obtained for the graphene samples with Ti/Au contacts. For the graphene samples without nanoparticles, Hall voltage varies linearly with the magnetic field (Figure 13a).
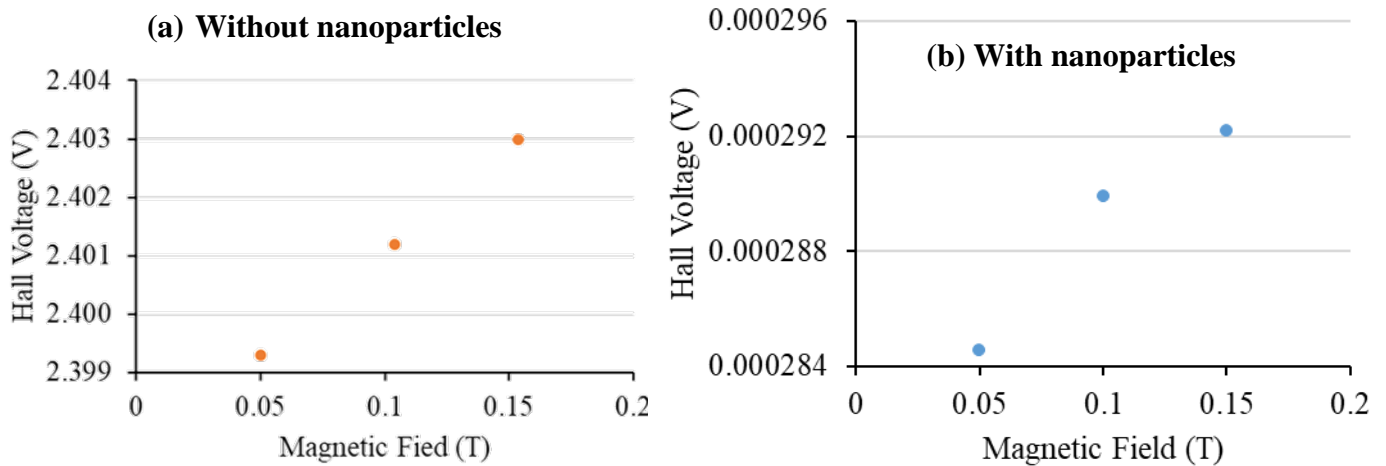

Figure 13. Hall measurements for monolayer graphene sample a) without and b) with nanoparticles.

After the initial measurement of bare graphene samples without nanoparticles, the sample was unmounted from the chip carrier and ZVI (zerovalent iron) nanoparticles were spray coated on using a spray coating mask and a hand-held air brush connected to a nitrogen flow (Figure 14). Hall measurements for the graphene samples with nanoparticles were done following the same procedure used for graphene samples without nanoparticles. As shown in Figure 13b, Hall voltage varies linearly with the magnetic field for the graphene sample with nanoparticles. It is important to note that the Hall voltage measurements are significantly lower for the monolayer graphene
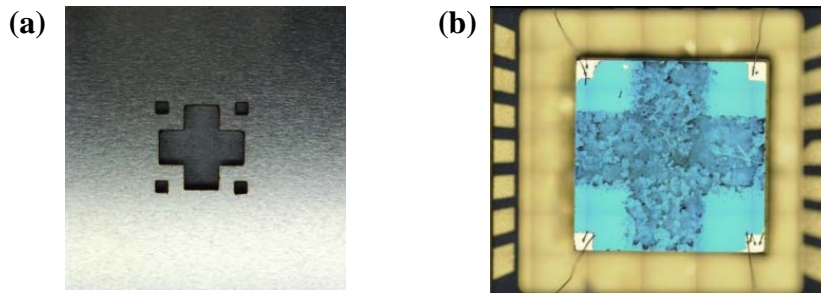

Figure 14. Nanoparticle deposition on graphene a) Mask design for nanoparticle deposition b) Nanoparticles deposited onto graphene oxide film on Si/SiO$_2$ wafer by spray coating.

sample after deposition of nanoparticles compared to the bare samples due to the high nanoparticle density loading of the sample.

Since there is a linear relationship between the magnetic field and the Hall voltage for the monolayer graphene sample (with and without nanoparticles) with Ti/Au contacts, we were able to calculate the mobility and carrier concentration using these data. However, the results for the nanoparticle-immobilized graphene sample are preliminary and require further optimization and tuning of the sample preparation approach to delineate effects of nanoparticle density from effects of sample preparation.

2.3. Calculation of Electron Mobility and Electron Carrier Concentration for Monolayer Graphene Sample

2.3.1 Theory

The theory used to calculate electron mobility and electron carrier concentration is based on the Van der Pauw setup (Figure 15).
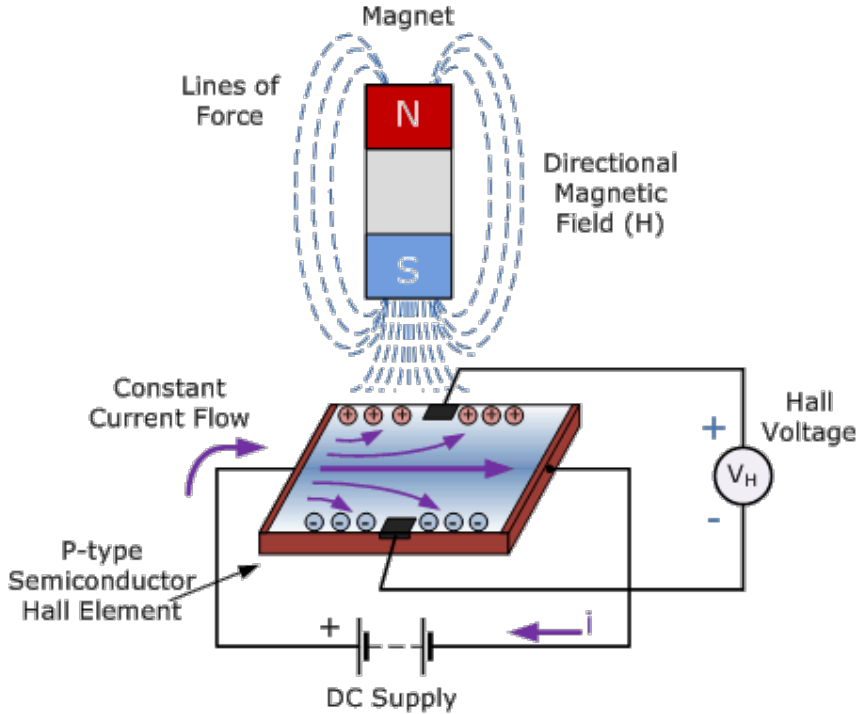

Figure 15. Schematic representation of the Van der Pauw setup for Hall voltage measurement illustrating movement of electrons to one side of the sample. This accumulation of electrons is measured as the Hall voltage.

In this setup, a conductor carries a current I, which is placed in a magnetic field, B. A negative charge carrier (electrons) travels to one side of the sample with a drift velocity, v_d. The force, F_B, that the electrons experience due to the magnetic field, B, and charge, q, is equal to:

$$\vec{F_B} = q\vec{v} \times \vec{B} \tag{4}$$

According to the right-hand rule, this force is perpendicular to the direction of the magnetic field and, drift velocity, and the position of the magnetic field and direction of the current control on which side of the sample the electrons accumulate (Figure 16).

$$|F_B| = e|v_d||B| \sin 90° = ev_dB \tag{5}$$

When charges build up on the opposite sides of the sample, an electric field, E, and associated force, F_E, evolve.

$$\vec{F_E} = q\vec{E} = eE \tag{6}$$

11

Therefore, now the net force (Lorentz force), F_{net}, can be given as,

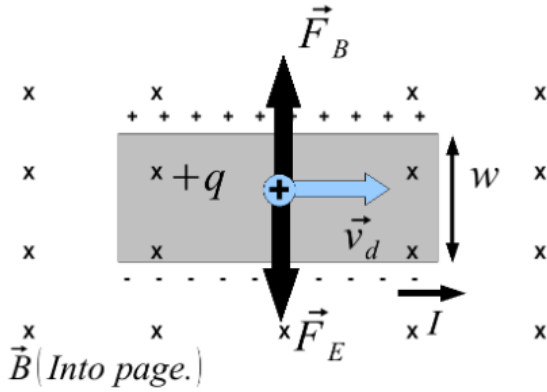$$F_{net} = F_E + F_B \qquad (7)$$

Figure 16. The forces on a positively charged particle in a magnetic field and induced electrical field.

However, at steady state,

$$F_E = F_B \qquad (8)$$

$$eE = ev_d B \qquad (9)$$

$$E = v_d B \qquad (10)$$

If the width of the sample is w, the Hall voltage (V_H) is equal to:

$$V_H = \Delta V = Ew = v_d Bw \qquad (11)$$

where w is the width of the sample, and ΔV is the measured voltage difference across the two electrodes.

If, J is current density, A is the cross-sectional area, w is the width of the sample, t is the thickness of the sample, n is the number of charge carriers per unit volume (i.e., concentration), e is the charge of the carrier, and L is the sample length, then:

$$J = \frac{I}{A} = \frac{I}{wt} = \frac{env_d A}{wt} = env_d \qquad (12)$$

$$\frac{V_H}{I} = \frac{v_d Bw}{env_d A} = \frac{v_d Bw}{env_d wt} = \frac{B}{ent} \qquad (13)$$

$$V_H = \frac{BI}{ent} \qquad (14)$$

$$n = \frac{BI}{eV_H t} \tag{15}$$

The Hall coefficient, R_H, can be written as:

$$R_H = \frac{1}{ne} = \left(\frac{V_H}{B}\right)\frac{t}{I} = \left(\frac{V_H}{I}\right)\frac{t}{B} \tag{16}$$

$$n = \frac{1}{eR_H} \tag{17}$$

R_H is related to the mobility (μ_m) according to the following equation where r is the resistivity.

$$\mu_m = \frac{R_H}{r} \tag{18}$$

Where:

$$r = \frac{V_H wt}{IL} \tag{19}$$

2.3.2 Calculations

Mobility and carrier concentration were calculated using equation 16, 18 and 19 shown above.

	Mobility (cm^2 V^{-1} s^{-1})		Carrier Concentration (cm^{-2})	
Magnetic field (T)	with NP	without NP	with NP	without NP
0.05	2.0×10^5	2.0×10^5	0.549×10^{13}	0.651×10^6
0.10	1.0×10^5	0.96×10^5	1.08×10^{13}	1.35×10^6
0.15	0.67×10^5	0.65×10^5	1.60×10^{13}	2.00×10^6
Average	**1.2×10^5**	**1.2×10^5**	**1.08×10^{13}**	**1.34×10^6**

Room temperature mobilities of graphene are typically in the range of ~10^4 cm^2 V^{-1} s^{-1} and the carrier concentrations are typically in the range of ~10^{12} cm^{-2}.[1] Although the mobility values obtained in this study, especially in the absence of nanoparticles, are close to the values reported in literature, carrier concentrations are six orders of magnitudes lower than the previously reported values.   Further, the mobility of charge carriers is the same in the presence and absence of nanoparticles while the carrier concentration in the presence of nanoparticles is nine orders of magnitude higher than the bare graphene sample. Also, the hall voltage values obtained for the sample with ZVI nano particles were close to zero. This reduces the reliability of the values of mobility and carrier concentrations obtained from calculations for the graphene sample with nanoparticles. One possible reason for this type of observation is a short circuiting of the Hall current by high density of nanoparticles. The problem was not anticipated in the experimental setup for nanoparticle deposition and thus would need to be addressed through sample optimization. One of the next steps in this work would be to optimize nanoparticle density and distribution in order to solve this problem.

References

1. Chen, J.; Jang, C.; Xiao, S.; Ishigami, M.; and Fuhrer, M.S., Intrinsic and Extrinsic Performance limits of Graphene Devices on SiO_2, *Nature Lett*., 2008, DOI:10.1038/nnano.2008.58.